



## Research papers

# High stability of autochthonous organic matter in inland aquatic ecosystems

Fan Xia<sup>a,b,c</sup>, Zaihua Liu<sup>a,c,d,\*</sup>, Min Zhao<sup>a,c</sup>, Haibo He<sup>a</sup>, Qiufang He<sup>e,f</sup>, Chaowei Lai<sup>a</sup>, Xuejun He<sup>a,b,c</sup>, Zhen Ma<sup>a</sup>, Yang Wu<sup>a</sup>, Song Ma<sup>a</sup>

<sup>a</sup> State Key Laboratory of Environmental Geochemistry, Institute of Geochemistry, CAS, Guiyang 550081, China

<sup>b</sup> University of Chinese Academy of Sciences, Beijing 100049, China

<sup>c</sup> Puding Karst Ecosystem Research Station, Chinese Ecosystem Research Network, CAS, Puding 562100, China

<sup>d</sup> CAS Center for Excellence in Quaternary Science & Global Change, Xi'an 710061, China

<sup>e</sup> Chongqing Key Laboratory of Karst Environment & School of Geographical Sciences, Southwest University, Chongqing 400700, China

<sup>f</sup> Key Laboratory of Karst Dynamics, Ministry of Nature Resources/Guangxi, Institute of Karst Geology, Chinese Academy of Geological Sciences, Guilin 541004, China



## ARTICLE INFO

## Keywords:

Recalcitrant dissolved organic matter  
CDOM  
Inland carbon sink  
Sediment

## ABSTRACT

Recalcitrant dissolved organic matter (RDOM) is a key component of ocean carbon sinks and it can be preserved in seawater for thousands of years. However, the fate of RDOM derived from the primary production in inland lake is unclear. In this study of Erhai lake in China, used the combination of  $\delta^{13}\text{C}$ , carbon/nitrogen (C/N) ratio, and optical spectroscopy analyses to constrain the variation of organic matter in the vertical direction (i.e., lake water  $\rightarrow$  trap sediments  $\rightarrow$  surface sediments  $\rightarrow$  core sediments), to trace the burial process of RDOM. Two autochthonous components (C1, C2) and two allochthonous components (C3, C4) were identified in the water. High concentrations of C2 in winter and spring indicate that these two seasons provide favourable burial conditions for autochthonous dissolved organic matter. Three autochthonous components (C1, C2, C5) and three allochthonous components (C3, C4, C6) were identified in the sediments. The contributions of autochthonous organic matter were  $\sim 49.9 \pm 5.84\%$  (based on PARAFAC analysis) and  $\sim 56.7 \pm 5.62\%$  (based on the C/N ratio) in the sediment trap samples;  $43.4 \pm 8.84\%$  (based on PARAFAC analysis) and  $40.8 \pm 14.26\%$  (based on the C/N ratio) in the surface sediments; and  $44.5 \pm 14.4\%$  (based on PARAFAC analysis) and  $48.4 \pm 6.04\%$  (based on the C/N ratio) in the core sediments. Additionally, C2, which is the autochthonous component after microbial mineralisation, was preserved as a significant part of the RDOM in the water. Our results suggest that the mineralisation of autochthonous organic matter (OM) in the core sediments did not promote bacterial mineralization, and that the burial of OM on long timescales depends primarily on its concentration rather than on its origin. Our results provide a new perspective for studying the stability of autochthonous OM and highlight a new direction for the study of the carbon sink of inland lakes.

## 1. Introduction

Intensifying human activities have led to significant increases in atmospheric greenhouse gases and hence in global temperatures (Feely et al., 2009; Javadinejad et al., 2019; Talebmorad and Ostad-Ali-Askari, 2022), resulting in an increase of the primary production of inland lakes (Hamdan et al., 2018; Liu et al., 2021; Visser et al., 2016). Studies of the associated organic carbon (OC) sequestration are vital for understanding the global carbon cycle, it has been shown that the annual OC sequestration of inland lakes is higher than that of marine ecosystems (Cole

et al., 2007; Liu et al., 2017; Tranvik et al., 2009). However, it remains unclear whether fixed carbon can be preserved over a long timescale, or whether it is used and transformed by planktonic bacteria, leading to the persistence of OC. Organic matter (OM) is typically used as a reliable proxy for OC. Exploring the processes involving the transfer of OM from the water column to the sediments can help understand the mechanisms of the mineralisation and burial of dissolved OM (DOM) in lakes.

Previous studies of ocean carbon sinks concluded that fluorescent DOM is produced in-situ within the ocean, as DOM is biologically oxidised and resistant to biological degradation on centennial to millennial

\* Corresponding author at: State Key Laboratory of Environmental Geochemistry, Institute of Geochemistry, CAS, Guiyang 550081, China.

E-mail address: [liuzaihua@vip.gyig.ac.cn](mailto:liuzaihua@vip.gyig.ac.cn) (Z. Liu).

time scales, and its in-situ production is greater than the riverine input of terrestrial humic substances (Yamashita and Tanoue, 2008). For example, the fluorescent signal of autochthonous DOM (auto-DOM) from picocyanobacteria persists in the deep ocean (Zhao et al., 2017), and its apparent age was determined to be  $\sim 6,000$  years. As the primary products of aquatic organisms, auto-DOM in inland water bodies undergoes a series of microbial consumption processes similar to those in the ocean. If the products or derivatives of auto-DOM after consumption produce recalcitrant dissolved OM (RDOM), this will contribute significantly to inland carbon sinks. We found that the auto-DOM mineralised by planktonic bacteria possesses several of the characteristics of RDOM at the Shawan Karst Water Carbon Cycle Test Site, Southwest (SW) China (Xia et al., 2022). However, the location of this components of the DOM in inland waters is still unknown. There is a growing consensus that organic molecules are not inherently labile or recalcitrant based solely on their chemical structures. Rather, a molecule's reactivity depends heavily on environmental conditions, such as the microbial community composition and activity, redox state, mineral associations, and the accessibility of substrates to microbes and their enzymes (Schmidt and Torn, 2011; Dittmar, 2015). The transport of DOM through the water column into the sediments could be an important pathway for OC accumulation in sediments (Tranvik et al., 2009; Wang et al., 2021; Nafchi et al., 2021), and previous studies have indicated that RDOM flocculates with iron and other metals to promote the burial of stable OC (Schmidt et al., 2009). Most of the autochthonous RDOM in inland water bodies may contribute to carbon sinks if it can be adsorbed by minerals and stored in the sediment as particulate OM (POM). This conjecture requires a search for evidence in the water column of inland

water bodies.

Previous studies used the measurements of  $\delta^{13}\text{C}$  and carbon/nitrogen (C/N) ratios to trace the source of organic matter. However due to the complexity of the end-members, the role of auto-DOM in the carbon cycle has been ignored. Additionally, such methods have often been used to determine the source of POM in water, and the source and destination of DOM could not be identified. As a reliable OM tracer technology, fluorescence spectroscopy has been used to identify the composition and origin of OM in water bodies. For example, Guillemette et al. (2017) explored the sedimentation and burial of OM in a Swedish lake by using fluorescence spectra with parallel factor analysis (PARAFAC), combined with C/N ratios, but they did not link the DOM in the water column with the sedimentary OM in series (Kothawala et al., 2014). This critical gap in lake carbon budgets needs to be urgently filled, and the relative contributions of allochthonous and autochthonous OM buried within lake sediments needs to be quantified (Hanson et al., 2014). Few attempts have been made to identify auto-DOM in the water column and to trace its burial in the sediments of inland water bodies. Discrete studies of the variations of OM in water and sediments cannot fully elucidate the stability of the different types of OM. In a previous study of Erhai Lake in China, we used fluorescence spectrum technology combined with two traditional geochemical parameters ( $\delta^{13}\text{C}$  values and C/N ratio), to characterize the local end-member substances and to select appropriate metrics to explore the origin of OM compositions from the water column to the lake sediments. Our objectives were to explore the vertical variation of OM from the water column to the sediments of an inland lake, and to determine if any recalcitrant OM was retained and if so to quantify its contribution to the

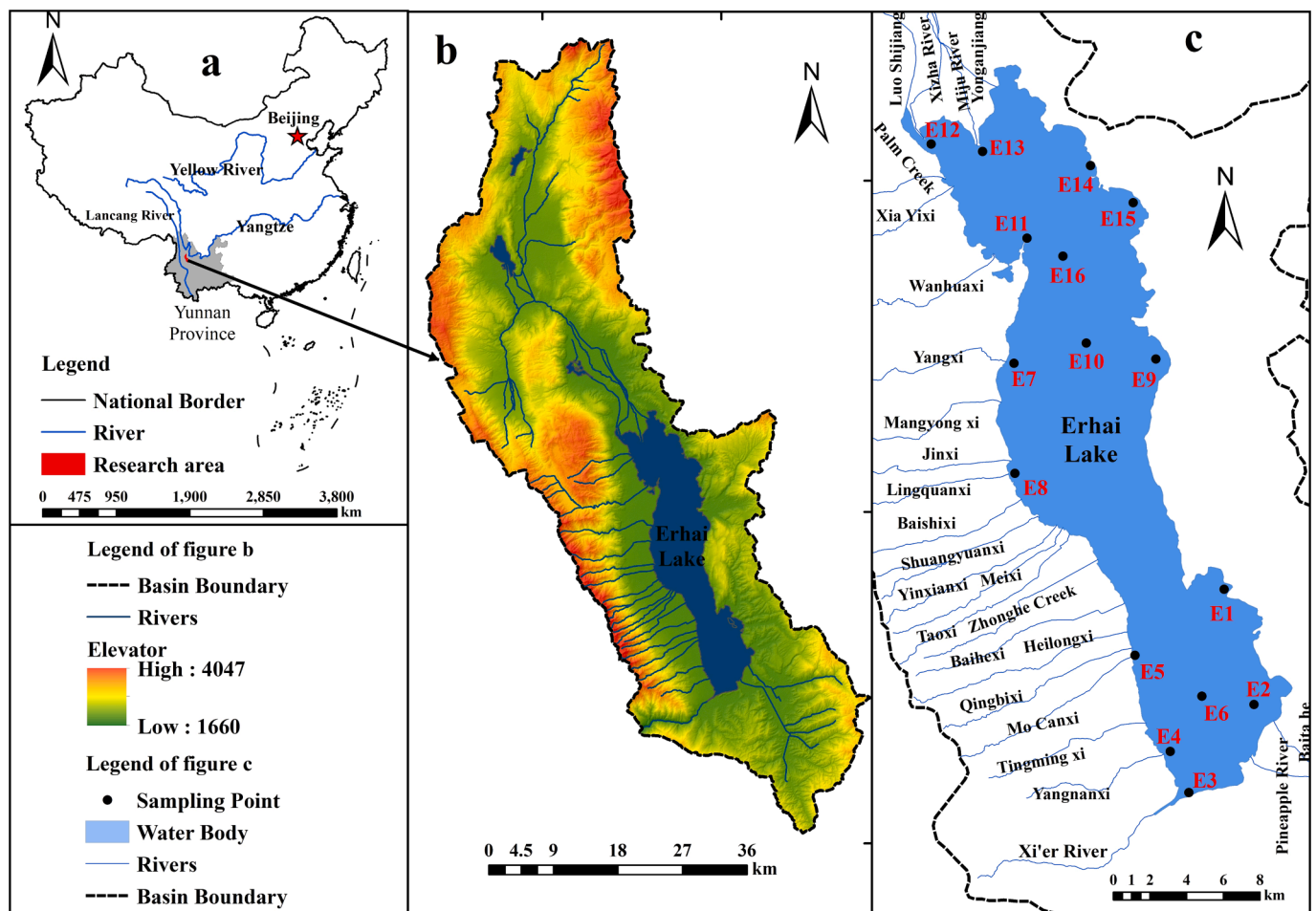


Fig. 1. Location of Erhai Lake in China and the sampling sites.

sediments. We also sought to determine the stability of autochthonous OM over a long timescale in inland lakes.

## 2. Materials and methods

### 2.1. Study area

Erhai Lake (25° 36′–25° 58′ N, 100° 5′–100° 18′ E) lies within Dali City, Yunnan Province, China (Fig. 1a); Dali City is noted for agriculture and tourism. The altitude of the lake surface is ~1973.7 m, the area is 249.8 km<sup>2</sup>, and the maximum water depth is 20.7 m (Fig. 1b). This area has the typical seasonal climate of a low-latitude plateau in this region, with the annual average rainfall of 1033 mm, and annual average temperature of 15.1°C. The rainfall is concentrated in summer and autumn (May to October), with the lowest precipitation in winter and spring (December to April). The wind speed is at a maximum in winter and spring. In summer and autumn, the water temperature and light level are sufficient for algal growth. The main surface inflows to Erhai lake are the northern Miju River and 18 streams from the Cangshan Mountains. Submerged plants are abundant in the shallow-water areas.

### 2.2. Sampling

Water samples were collected seasonally in July and October 2020, and January and April 2021. Sediment and core samples were collected in October 2020. Water and sediment samples were obtained from 16 stations within the lake, and sediment cores were collected from the deepest site (site E10, 20 m water depth) (Fig. 1c). Three sediment traps devices (sites E10, E12, E16) were emplaced and remained in position for four months (from April to July 2021). Each trap was located 5 m, below the surface; however, the trap at the coring site (E10) was added 15 m below the surface.

A multiparameter water quality probe was used to measure the water temperature (T), pH, and dissolved oxygen (DO). Dissolved inorganic carbon was titrated in the field using an Aquamerck alkalinity test kit with an estimated accuracy of 6 mg/L. Dissolved CO<sub>2</sub> (CO<sub>2</sub> (aq)) concentrations were calculated using Phreeqc (Zeebe and Wolf-Gladrow, 2001). The water samples (300 ml) were filtered through a 0.7-μm membrane; 150 ml was stored in brown glass bottles at 4 °C to measure the dissolved organic carbon (DOC) content, and the remaining 150 ml was filtered through a 0.22-μm membrane for excitation-emission matrix (EEM) fluorescence analysis. The DOC concentration was measured with an OI Analytical “total inorganic carbon–total organic carbon (TIC–TOC)” analyser.

The sediment traps were open-topped cylindrical polyethylene tubes with a length of 105 cm and internal diameter of 15 cm (He et al., 2020). The trapped sediment was transferred to plastic containers in the field and stored at 4 °C. The trapped sediment samples were freeze-dried to a constant weight and homogenised for elemental analysis and DOM extraction.

Three sediment core were collected from the centre of the lake (site E10) using a gravity corer fitted with Perspex tubes with an internal diameter of 58 mm. The sediment core (76 cm long) was split into 2 cm intervals (0–12 cm) and then at 4 cm intervals (12–76 cm), transferred into pre-cleaned sterile centrifuge tubes (PE) immediately after collection, and freeze-dried in the laboratory.

### 2.3. Analytical methods

Freeze-dried trap and sediment samples were analysed using a gas isotope ratio mass spectrometer (EA-MAT253), with the conventional Vienna PeeDee Belemnite (VPDB) carbonate standard, to determine the δ<sup>13</sup>C<sub>org</sub>. δ<sup>13</sup>C is calculated as: δ<sup>13</sup>C<sub>sample</sub> = (R<sub>sample</sub>/R<sub>standard</sub>-1) × 1000; in this equation, R is the <sup>13</sup>C/<sup>12</sup>C ratio of the sample.

The relative contribution of aquatic versus terrestrial precursors to the sediment organic matter (OM) was estimated using the C/N

elemental ratio and the corresponding two-source mixing equations:

$$C/N = f_1 \times C/N_{\text{auto}} + f_2 \times C/N_{\text{allo}}$$

$$f_1 + f_2 = 1$$

where  $f_1$  and  $f_2$  are the relative contributions of autochthonous OM and allochthonous OM respectively. In this study, we assumed that the terrestrial and aquatic (microbially) derived average C/N ratio end-members of soil and phytoplankton were 12.37 and 7.39 respectively.

Total organic carbon (TOC), total nitrogen (TN) content, and TOC/TN (atomic) ratios were determined for the trap and core sediments using an elemental analyser, following acid treatment with 1.5 mol/L HCl for 24 h to remove inorganic carbon.

Sedimentary DOM was extracted following the procedure of Wolfe et al. (2002) for fluorescence analysis. The DOC of the extracted samples was determined using the OI Analytical “TIC–TOC” analyser. EEM fluorescence analysis was conducted using an RF-5301PC spectrophotometer (Shimadzu, Japan) equipped with a 150 W Xe lamp at the Chongqing Key Laboratory of Karst Environment & School of Geographical Sciences, Southwest University.

The excitation (Ex) spectra ranged from 220 to 500 nm at 5 nm increments, and the emission (Em) spectra ranged from 250 to 600 nm at 2 nm increments. All EEMs were calibrated to the water Raman signals (excitation 350 nm), and then the data were normalized to Raman units (R.U.). MATLAB R2017a and the DOMFluor toolbox were used to conduct the Parallel Factor (PARAFAC) analysis and to calculate the chromophoric DOM (CDOM) component factors. Raman and Rayleigh scattering were mitigated by subtracting the deionized water EEM spectrum collected from each corrected EEM and with Delaunay triangular interpolation. Outlier samples were eliminated by checking the component loadings and leverages of each sample. Split-half analysis and random initialization were used to validate the identified components (Stedmon and Markager, 2005). The PARAFAC component position was determined by the component F<sub>max</sub> value and its Ex and Em wavelength. The PARAFAC component percentages and position were used to determine the quantitative and qualitative variations in CDOM and DOM between water samples. We used PARAFAC analysis to independently identify the fluorescence spectral components of organic matter in water and sediment, and then analyzed four fluorescence signals of the organic matter components in water and six fluorescence signals of organic matter components in sediment. Finally, we calculated the fluorescence index (FI) and humification index (HIX) (Guillemette et al., 2016).

DataGraph was used to plot the data and to conduct linear regression analysis. A significance level of 0.05 was selected for multiple comparisons to test the null hypothesis. Linear correlations were considered statistically significant at  $p < 0.01$ .

## 3. Results

### 3.1. Seasonality of C/N ratio, δ<sup>13</sup>C<sub>org</sub> and DOM fluorescence properties of the lake water

The hydrochemistry of each water sampling site was similar, especially in winter and spring. The water temperature ranged from 15.59 to 25.36 °C, and the pH ranged from 7.76 to 9.36. DOC concentrations were similar in summer, autumn, and winter, with the mean of 5.41 ± 0.99 mg/L, but with a large increase in spring (20.24 ± 9.42 mg/L) (Fig. S1). The C/N ratio of POC ranged from 6.3 to 10.2. δ<sup>13</sup>C<sub>org</sub> showed a substantial seasonal variation and ranged from –21.8 to –29.1 ‰; the values were negative in winter and positive in the summer (Fig. S2).

Four EEM-PARAFAC components were identified (Fig. 2a). The ex|em wavelengths were 230(280)|326, 255|381(444), 275(340)|466, and 310|412 nm. Component C1 represents a tyrosine-like fluorophore (Zhou et al., 2019). Components C2, C3, and C4 represent humic- and fulvic-like fluorophores. Based on previous studies, Components C1 and

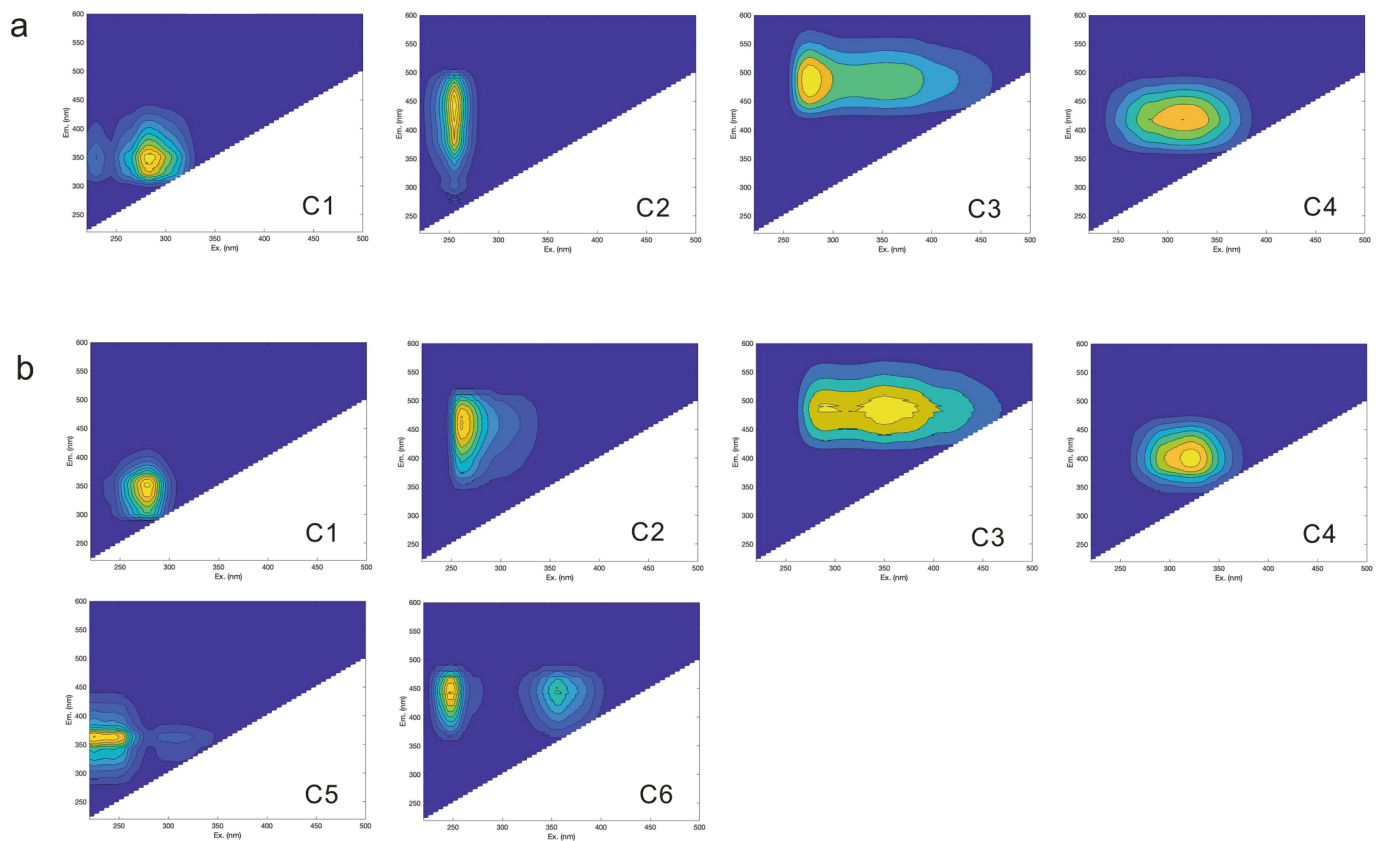


**Fig. 2.** Contour plots of EEM-PARAFAC components of DOM in (a) water and (b) traps and sediments. Component C1 represent tyrosine-like fluorophores; C2, C3, and C4 represent humic-like fluorophores in section a; C1 and C5 represent tyrosine-like fluorophores; C2, C3, C4, and C6 represent humic-like components in section b. The colours indicate the degree of fluorescence intensity under excitation and emission wavelengths.

C2 represent fresh auto-DOM in water and auto-DOM mineralised by microbes, respectively (Kida et al., 2019; Xia et al., 2021). Components C3 and C4 represent terrestrial humus-like DOM and allochthonous DOM (allo-DOM) mineralised by microbes, respectively.

We normalised the components by the DOC (Kida et al., 2019), and evaluated the correlations between  $F_{max}/DOC_{C1}$  and  $F_{max}/DOC_{C2}$ ,  $F_{max}/DOC_{C3}$ , and  $F_{max}/DOC_{C4}$  components in different seasons, respectively. The correlation analysis results showed that C1 had a significant relationship with C2 in summer and spring (Fig. 3a), and there was a significant correlation between C3 and C4 throughout the year (Fig. 3b). We considered that these findings reflect differences in the origin of the components.

The fluorescence indices, fluorescence index (FI), biological index (BIX), and humification index (HIX), showed seasonal variations (Fig. S4). The autumn water samples had higher HIX values, whereas the spring samples had higher FI values. The results showed that the contribution of allo-DOM was greater in summer, while that of autochthonous DOM was greater in spring. However, this is inconsistent with the photosynthetic intensity (water temperature and rainfall), which we suggest may be due to the concentration of organic matter is the water column following the two processes of photosynthesis and degradation. It increased to  $0.073 \pm 0.0068$  R.U L mg C<sup>-1</sup> in winter and was higher than the other three components in all seasons (Fig. 3c). C1 and C3 decreased to  $0.007 \pm 0.0048$  and  $0.007 \pm 0.0048$  R.U L mg C<sup>-1</sup> in spring, and remained at  $0.022 \pm 0.0060$  and  $0.025 \pm 0.0078$  R.U L mg C<sup>-1</sup> in other seasons, respectively. In the same season, there was little difference in the proportion of components at all the sites. This was manifested mainly by a higher proportion of allo-DOM in summer and autumn, and a higher proportion of auto-DOM in winter and spring (Fig. S3).

### 3.2. C/N ratio, $\delta^{13}C_{Org}$ , and fluorescence properties of the trap and surface sediments

In the trap sediments, the C/N ratio ranged from 9.19 to 9.79 (Table S1); at site E10 the sample from 5 m depth had a higher C/N ratio than the sample from 15 m depth. Additionally, the surface sediments had a higher average C/N ratio ( $\sim 10.11 \pm 0.69$ ) than the trap samples. However, the C/N ratio of surface sediments was lower than that of trap sediments at site E16. The  $\delta^{13}C_{Org}$  values of the trap samples ranged from  $-23.761$  to  $-26.536$  ‰. It showed that  $\delta^{13}C_{Org}$  value was lower in the deeper trap at site E10, and the  $\delta^{13}C_{Org}$  of the surface sediments was slightly lower than at site E10 (the sample from 15 m depth). The  $\delta^{13}C_{Org}$  values of the surface sediments at sites E12 and E16 ranged from  $-21.77$  to  $-27.77$  ‰, which were lower than those of the trap sediments.

FI values ranged between 1.0 and 1.8 in most of the trap and surface sediments (Fig. S4). The FI value of the trapped sediments at site E12 was 1.92, and that of the surface sediments at site E10 was 3.64, suggesting that auto-DOM accounted for most of the DOM. The HIX of the trap sediments was  $< 4$ , and the values of the five surface sediments ranged from 4 to 10, indicating that the organic material was strongly humified. The BIX of the trap sediments ranged from 0.74 to 0.97 (Fig. S4), indicating their autochthonous and microbial origin. The BIX of the surface sediments varied widely, but was mostly  $< 0.8$ , and was greatly affected by the OM.

Six EEM-PARAFAC components were identified in the sediments (Fig. 2b). Sedimentary OM had more components than water OM, with additional EEM components at  $ex|em$  wavelengths of C5 and C6 at 245|352, 250 (355)|451 nm. Components C1, C2, C3, and C4 are consistent with the fluorescence components in water. C5 represents tryptophan-like fluorophores (Wang et al., 2020) and C6 is a humic-like component (He et al., 2022). Based on previous studies (Liu et al., 2019; Kida



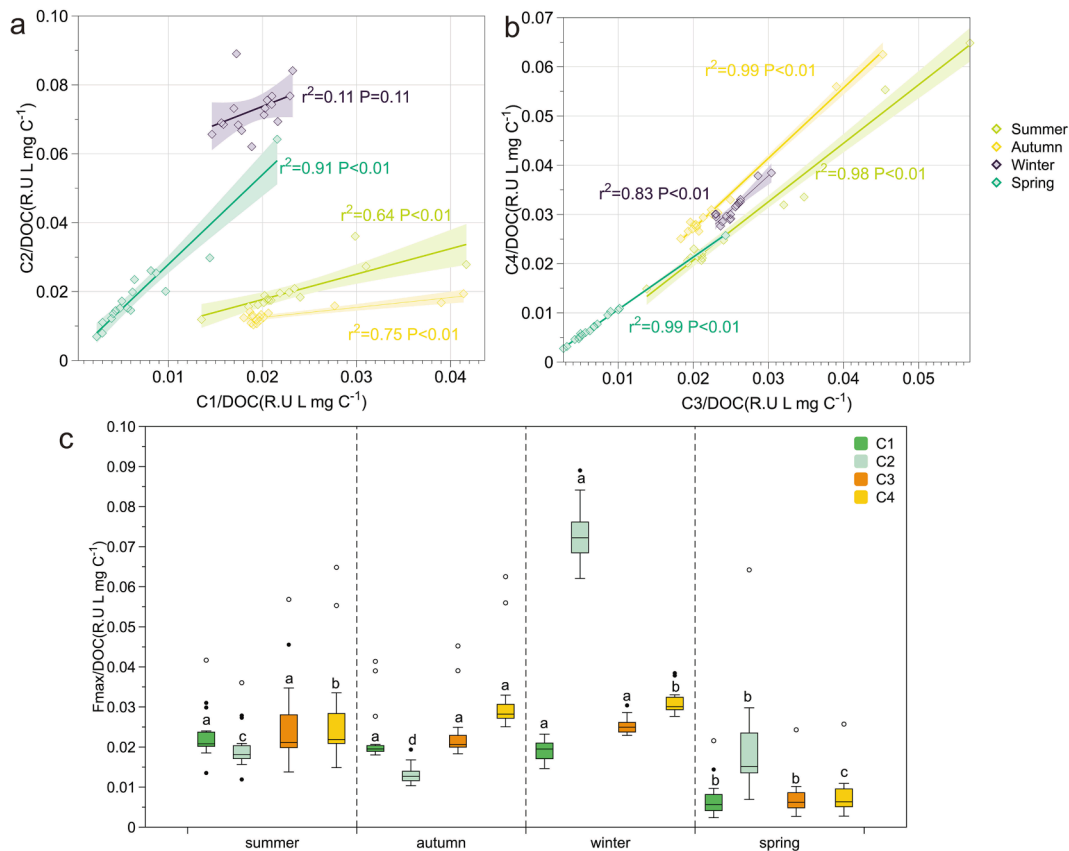


**Fig. 3.** Results of linear regression analysis of (a) fresh (C1 and C3), and (b) mineralised (C2 and C4) components from different sources. (c) Box plots summarizing the seasonal variations of the four components after standardisation; (one-way ANOVA with an LSD test,  $p < 0.05$ ). Different lowercase letters indicate that the same component varies significantly between different seasons).

et al., 2019; He et al., 2021), components C1, C2, and C5 in all the sediment samples represent OM formed by autochthonous production and transformation, whereas components C3, C4, and C6 represent OM supplied from terrestrial sources. Auto-DOM (C1 + C2 + C5) contributed  $49.9 \pm 5.84\%$  of the OM in the trap sediments, and its contribution to the surface sediments decreased slightly ( $\sim 43.4 \pm 8.84\%$ ) (Fig. 4a). The change of each component from the trapped sediments to the surface sediments can be obtained by subtracting the fraction of the trapped sediment component from the surface sediment component, which can characterise the vertical removal and sequestration of each component in the lake (Fig. 4b). We found that only components C1 showed a significant decrease ( $p < 0.01$ ), while components C2, C3, C5, and C6 all

increased slightly.

### 3.3. Stratigraphic changes in C/N ratio, $\delta^{13}C_{org}$ and fluorescence properties of the organic carbon in the core sediments

The C/N ratio of the core sediments ranged from 9.51 to 10.64, with an average of  $9.96 \pm 0.3$ ; the highest value was at the depth of 10–12 cm. The origin of the stratigraphic changes in the C/N ratio is complicated, being the result of different modes of bacterial utilisation of carbon and nitrogen within each layer. We divided the changes in the core into the following four stages according to the changes with increasing depth. Stage I: DOC and TOC decrease substantially from 2 cm (20.9 mg/L) to

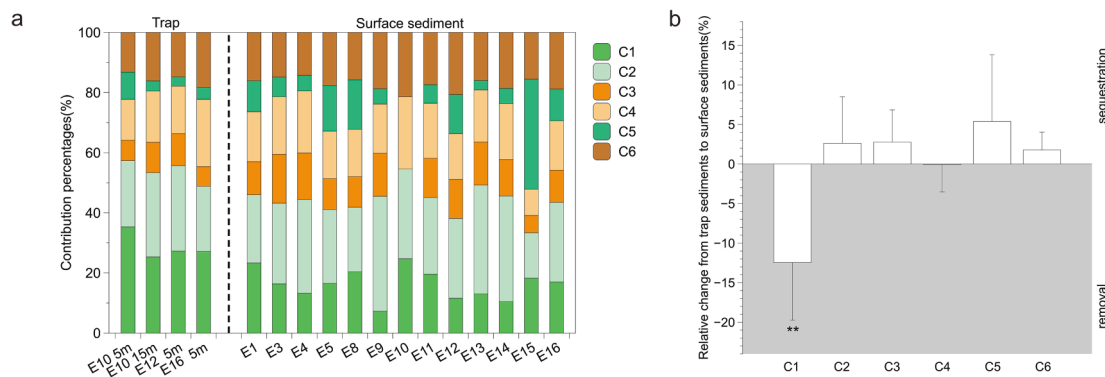


**Fig. 4.** Relative abundance of six fluorescence components in (a) trap and surface sediments, and (b) relative change of the six fluorescence components from the trap to the surface sediments. Positive values indicate higher values in the sediments than in the traps, indicating sequestration, whereas negative values indicate removal (shaded area). The bars represent averages  $\pm$  standard deviation (SD). Asterisks denote the significance levels of independent t tests (\*\*:  $p < 0.01$ ).

12 cm (3.82 mg/L), representing the main stage of OM degradation and the values then remain stable from 12 cm to the base of the core (Fig. 5a). The increase in the C/N ratios in this stage indicates that in addition to OC consumption, the utilisation of nitrogen in the upper core layers is consistent with the results of previous studies matter (Meyers, 1997; Wan et al., 2003). Stage II: the C/N ratio increases overall, and the  $\delta^{13}\text{C}_{\text{org}}$  values become slightly less negative with increasing depth (Fig. 5b). Stage III: the C/N ratio decreased, and the  $\delta^{13}\text{C}_{\text{org}}$  values become slightly more negative. Stage IV, the C/N ratios increase slightly and the  $\delta^{13}\text{C}_{\text{org}}$  values become negative. The  $\delta^{13}\text{C}_{\text{org}}$  values show a slight negative trend from the top (-27.40 ‰) to the bottom (-27.36 ‰) of the core, and  $\delta^{13}\text{C}_{\text{org}}$  decrease significantly from 0 to 8 cm in Stage I, with an average value of  $27.31 \pm 0.35$  ‰ (Fig. 5b).

The variations of FI in the core sediments are similar to those of BIX (Fig. 5c), showing a fluctuating pattern with the values ranging from 1.54 to 1.84, with most values were  $>1.2$  and  $<1.8$ . According to previous research, OM from both autochthonous and allochthonous sources is present throughout the core. BIX values range from 0.76 to 1.15 and show a slight fluctuation below the depth of 54 cm. Except for stage I, the variations of FI and BIX are consistent with those of the C/N ratio. HIX increased from the top to the bottom of the core, and the values remained stable in Stage IV. The variations of OM in stage I were minor, and the OM content remained at a very low level, indicating that the surface sediments may be greatly influenced by autochthonous OM.

We calculated the normalised maximum fluorescence intensities (Fmax/DOC) (Fig. 5e) and the relative contributions (%) of the six EEM-PARAFAC components (Fig. 5f). The results showed that the Fmax/DOC of tryptophan-like components C1 and C5 decreased within the core. Fmax/DOC of component C1 decreased from 0.045 to 0.012 R.U.L mg  $\text{C}^{-1}$ , whereas that of C5 reached 0.095 R.U.L mg  $\text{C}^{-1}$  and then gradually decreased to zero with increasing depth. Fmax/DOC of C2 component, another auto-DOM component, increased with depth to 0.055 R.U.L mg

$\text{C}^{-1}$ , and its trend of variation is essentially the opposite to those of C1 and C5. We have preliminarily determined that components C1 and C5 were gradually removed on a long time-scale, whereas component C2 has undergone sequestration. Fmax/DOC of component C3 fluctuates slightly throughout the core compared to that of the other components, with a large variation over 0–10 cm, and the values remained between 0.013 and 0.038 R.U.L mg  $\text{C}^{-1}$  below. The major fluctuations of Fmax/DOC of component C4 were also concentrated within the 0 and 10 cm depth interval, and then remained between 0.010 and 0.090 R.U.L mg  $\text{C}^{-1}$  with increasing depth. Component C6 represents a new humus component in the sediments, and its Fmax/DOC values ranged from 0.006 to 0.040 R.U.L mg  $\text{C}^{-1}$ , with a large variation within the 0–10 cm depth interval with additional large fluctuation within the 10–40 cm interval.

In terms of their relative proportions, components C1 and C5 accounted for 23.4 % and 28.0 % at the top of the core, respectively, decreasing to 6.1 % and 0 % at the bottom, while, the contribution of C2 increased from 13.3 % to 25.2 % from the top to the bottom of core sediments. Regarding the contribution of allochthonous components, the proportions of components C3, C4, and C6 increased from 7.4 %, 13.6 %, and 14.3 % to 17.3 %, 38.4 %, and 12.2 %, respectively, with C4 showing the largest increase.

## 4. Discussion

### 4.1. Vertical variations of the organic matter indices in Erhai lake

Based on the potential end-member values (terrestrial plants, phytoplankton, soil, and submerged plants) (Meyers and Ishiwatari, 2003; Lamb et al., 2006), the  $\delta^{13}\text{C}_{\text{org}}$  values of the surface sediments were even more positive than those of the trap sediments (Fig. 6a). This may be related to the greater impact of submerged plants on the surface

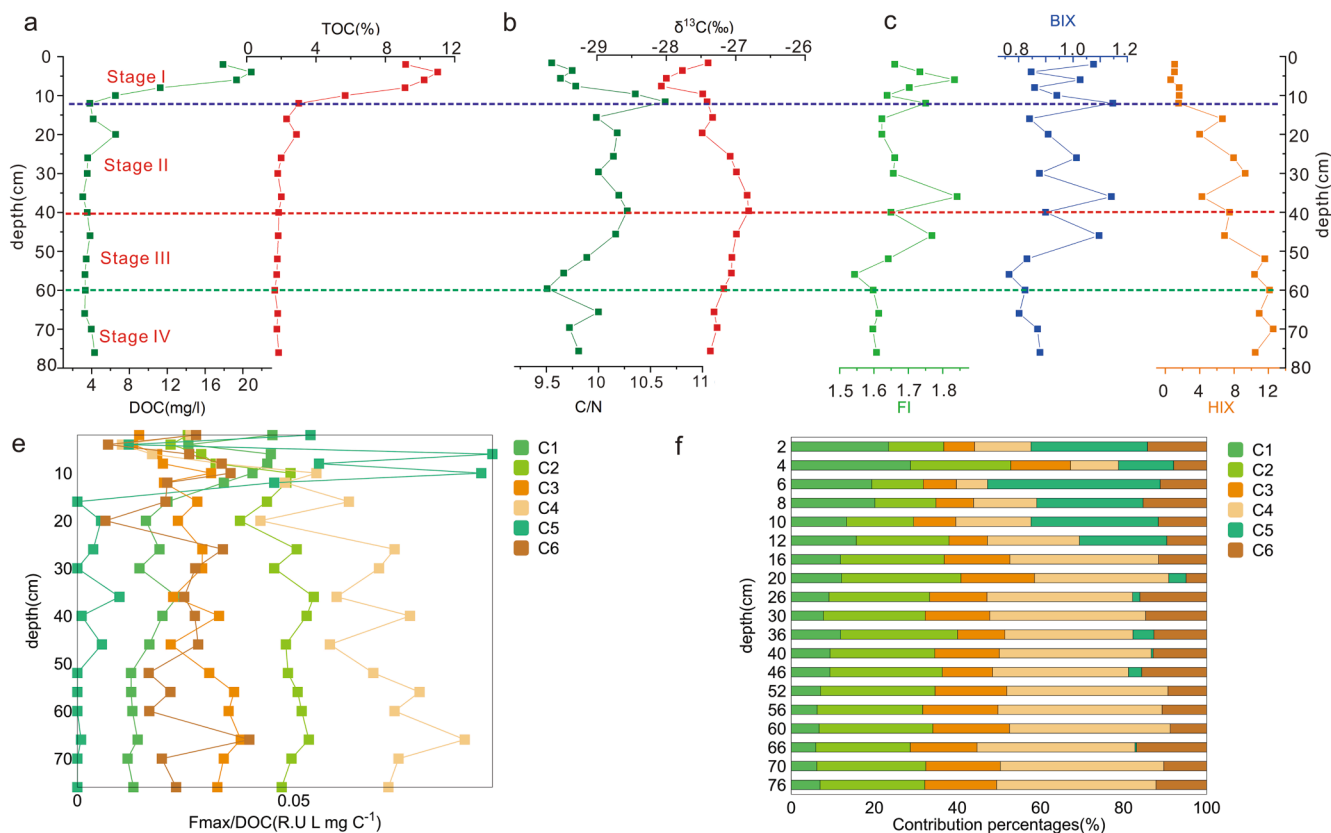


**Fig. 5.** Profiles of organic matter correlation index and six EEM-PARAFAC components in the core sediments: (a) concentration of OC, (b) C/N ratio and  $\delta^{13}\text{C}_{\text{org}}$ , and (c) the fluorescence index of the core sediments. (d) Fmax/DOC of the CDOM and (e) percentages contributions of the CDOM.

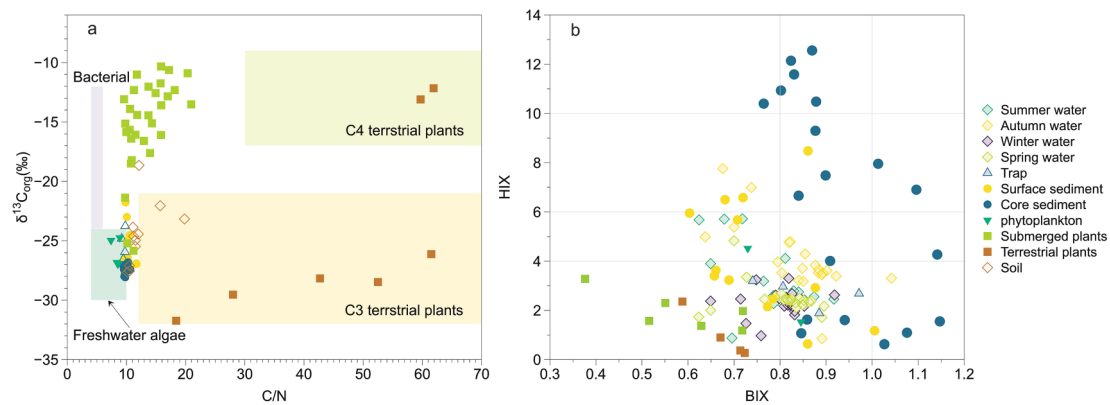


**Fig. 6.** Variations of (a)  $\delta^{13}\text{C}_{\text{org}}$  and C/N ratio and (b) fluorescence indices for Erhai Lake. The points represent the measured values obtained by sampling, and the rectangles represents the value obtained from the literature. The value of (a)  $\delta^{13}\text{C}_{\text{org}}$  and C/N ratio of submerged plants are greatly affected by the environment; thus, the values from the literature are not shown in (a).

sediments because submerged plants had more positive  $\delta^{13}\text{C}_{\text{org}}$  values in our study ( $-25.84$  to  $-10.34$  ‰). According to the data summarised by Hassan et al. (1997) and Meyers and Ishiwatari (2003), the algal  $\delta^{13}\text{C}_{\text{org}}$  values ranged from  $-32$  to  $-24$  ‰. The  $\delta^{13}\text{C}_{\text{org}}$  values in the core sediments were more negative than those of the trap sediments, indicating that more algae-derived OM was preserved in the core sediments. The C/N ratios of the soils were very low and deviated from those of terrestrial plants. Microbial mineralisation is a carbon-consuming process, and soil is a product of terrestrial plant litter following microbial, physical, and chemical mineralisation (Lehmann et al., 2002). The input of terrestrial OM is mostly in the form of soil; thus, the C/N ratio of soil is more suitable as an end-member of terrestrial OC. In addition, the C/N ratios in the water ( $<10$ ) were lower than in those sediments, with the values of the former closer to those of planktonic algae. Although, part of the autochthonous OM is inevitably utilized by the planktonic bacteria, together with the sedimentation process, the organic matter produced by aquatic photosynthesizing organisms still makes a large contribution to the sediments (He et al., 2020).

The HIX values of submerged and terrestrial plants indicate weak humification, and the submerged plants had higher HIX values than the terrestrial plants (Fig. 6b). The recalcitrance of OM is usually assessed by the degree of humification, because humification usually represents the extent to which OM is utilized by bacteria (Zhou et al., 2021). Submerged plants, as an important part of autochthonous production, may eventually have an OM content similar to that of terrestrial plants preserved as part of the carbon sink. Previous studies found that terrestrial plants have a large amount of low-molecular OM and are preferentially consumed and incorporated into the biomass by bacteria (Hobbie, 1988; Guillemette et al., 2016), and the recalcitrant OM imported into the lake tends to be a degradation product of terrestrial plants. This suggests that autochthonous OM may also contain recalcitrant components that can be preserved in the sediments. Therefore, previous researchers may have inadvertently assumed that fresh autochthonous OM was more easily degraded than the imported allochthonous OM. It is necessary to pay more attention to the stability of the degraded products, rather than only focusing only on the freshly generated substances. Although the vertical changes in the HIX values from the lake water to the sediment are more complex, there is an overall increasing trend. Most of the HIX values of the upper part of the core and the surface sediments were low, possibly because of the incomplete degradation of the submerged plants incorporated in the surface sediments. The BIX values of soil, terrestrial plants, and submerged plants were low (generally  $<0.8$  suggesting a terrigenous attribute), indicating that submerged and land plants are very similar, which has a major effect on the surface sediments. The BIX values of the water and most of the sediments were  $>0.8$ , indicating the large contribution of autochthonous OM, which is consistent with the conclusions based on the  $\delta^{13}\text{C}_{\text{org}}$  and C/N values. Combined with results

of the four indicators ( $\delta^{13}\text{C}_{\text{org}}$ , C/N, HIX, BIX), the terrestrial characteristics of some of the surface sediments may be the result of the incorporation of incompletely degraded submerged plants.

All our measured indices from the core sediments show that when the OC content remained stable after stage I, the changes in the C/N ratios and fluorescence indices (HIX and BIX) were consistent, which was also observed in previous research (Guillemette et al., 2016). The main cause of the variation of these indicators is their different origins (Filippi and Talbot, 2005; He et al., 2020), and the variation of  $\delta^{13}\text{C}_{\text{org}}$  also demonstrates this. The OC content in the sediment core stabilised at  $2.02 \pm 0.43$  %, and the proportion of each fluorescence component remained constant in the lower sediment layers, regardless of their origin. This suggests that in the nutrient-poor environment of the stable layers, the main limiting factor for microbial degradation may not be the origin of the OC but rather its concentration. It has been found that the bacterial abundance in sediments is positively related to the concentration of sedimentary OM and bacterioplankton niche partitioning in the use of phytoplankton-derived DOC; thus, quantity is more important than quality (Schallenberg and Kalf, 1993; Sarmento et al., 2016). Hence, when the OM concentration is below the threshold for prokaryotic utilization in the deep layers of the sediments, OM will no longer be utilized, excluding the influence of redox conditions. This conclusion agrees with the dilution limits of C utilization in the deep ocean (Arrieta et al., 2015). Regardless, in future research on inland lakes it may be appropriate to reevaluate the importance of OM degradation away from its origin (autochthonous and allochthonous) and towards its concentration.

#### 4.2. Identification and burial of autochthonous RDOM in lake sediments

RDOM has been regarded as the product or derivative of OM generated by primary production in the ocean and proposed as a microbial carbon pump (MCP) (Longhurst and Harrison, 1989; Jiao et al., 2014; Legendre et al., 2015). An increasing number of studies have indicated that the formation of RDOM is associated with the utilisation of transformed products by planktonic bacteria in water, and that microorganisms tend to transform DOM from relatively high ( $>400$  Da) to low ( $<400$  Da) molecular weight compounds corresponding to increasing aromaticity (Chen et al., 2021). The component C2 characteristics in our study are similar to the RDOM in the ocean in our study. We found that the relationship between C2 and planktonic bacteria indicates its RDOM properties (Xia et al., 2022). This component has been reported as a humic-like fluorescence peak in algal culture experiments (McIntyre and Gueguen, 2013) and was independent of the catchment area in continental Antarctica (Kida et al., 2019). The relationship between C2, protein-like components, and DIC has been observed in karst aquatic ecosystems (He et al., 2021), and a significant correlation

between C2 and chlorophyll has been found in river-estuary transects (namely, in the Liao and Daliao rivers in Northeast China (He et al., 2022)). We compared the molecular compositions of the C1 (similar to C5 reported in He et al (2022)) and C2 (similar to C3 reported in He et al (2022)) fluorescence components in our study, as determined by Fourier-transform-ion cyclotron resonance mass spectrometry (FT-ICR MS). This showed that the two autochthonous components have a similar inheritance and were significantly different to the allochthonous humus (which was similar to the C1, C2, and C4 component reported in He et al (2022)). Previous studies have identified C2 as an autochthonous degradation product, but its long-term stability in inland aquatic systems has not been studied. Based on the above studies, the significant relationship in lake water in spring and summer, and the consistent trends of variation trends between components C1 and C2 in the core sediments, further underlines their autochthonous characteristics. C2 was regarded as a photo-recalcitrant humic-like component because of the rapid attenuation of ultraviolet-B (UVB) light in water (Stedmon and Markager, 2005). We found that the proportion of C2 generally increases in the vertical direction (i.e., from the lake water to increasing depth within the sediments) (Fig. 7). Therefore, the average proportion of C2 in the surface sediments was higher than that in the upper part of the sediment core because of the accumulation of fresh OM (components C1 and C5) in the surface layer of the core located in the centre of the lake. In the middle and bottom layers of the core, with decreases in C1 and C5, the proportion of C2 gradually increased to a maximum. All these observations highlight the recalcitrant characteristics of component C2.

The proportion of component C2 was higher in winter and spring, which is consistent with the seasonal changes in the Lijiang River (He et al., 2021). Samples from the DaLiao River taken during winter showed a higher proportion of C2 (He et al., 2022). We consider that the decay of submerged plants in winter releases a large amount of autochthonous OM mineralised by bacteria, leading to the gradual accumulation of component C2. The decreased rainfall in winter results in less allochthonous OM being imported to the lake; thus, the proportion of C2 in all components increased significantly. Despite the intense primary photosynthesis in summer and autumn, the high microbial activity and increase in the lake sedimentation flux results in the consumption of part of the C2 component (Gudasz et al., 2012), or in its rapid burial in the sediments (Guillemette et al., 2016). The high discharge during the two seasons and the large amount of allochthonous input also contributed to the low proportion of C2. The stability of C2 is only a relative concept, as

Dittmar (2015) proposed that extreme substrate dilution is a stabilisation mechanism and suggested that DOM stability may be independent of the molecular structure. Owing to the relative stability of component C2, a high proportion of C2 was stabilised in the lake in winter and spring. Therefore, these two seasons may be the optimum times for the burial of C2 (Dittmar, 2015). The proportion of C2 gradually increased in the sediments and eventually stabilised at ~37%. Although we have not monitored the increase in long-term RDOM in inland lakes, as was done in the ocean (Jiao et al., 2010), we found that large amounts of RDOM were present at the bottom of the sediment core, compared to the other components. The C2 component and the C/N ratio were uncorrelated in the water and in the core sediments ( $p > 0.05$ ) (Fig. S6). We suggest that C/N ratio reflects both carbon consumption and nitrogen use, which makes its interpretation somewhat difficult.

To further explore the contribution of these stable components at different depths within the lake and sediments, we calculated  $F_{max(C2/C1+C2+C5)}$  and  $F_{max(C4/C3+C4+C6)}$  in the water, trap sediments, surface sediments, and core sediments (Table S2 and Fig. S2) to characterise the stability rate of the two OM sources (Xia et al., 2022). The results showed that the stability rate of the autochthonous OM had seasonal differences, which is similar to the results obtained in water at the Puding karst Simulation test site (Xia et al., 2022). It is noteworthy that the stability rate of autochthonous OM in Erhai Lake during summer and autumn was higher than that at the Puding Simulation Test site (Table S2), which is related to the longer retention time of water in Erhai Lake (about 2.75 a) (Zhao et al., 2020). The longer retention time results in the accumulation of C2 in the water, resulting in the greater stability rate of the autochthonous OM. Although we are unable to detect the presence of recalcitrant OM in Erhai lake based on its  $^{14}C$  age (as is possible in the oceanic research; Hansell et al., 2012), comparison of the stability rate of autochthonous OM in the two regions further confirms our understanding of the recalcitrant nature of component C2 (Fig. S7). Additionally, the results indicated that the autochthonous stability rate increased with sediment depth. The high stability rate is consistent with the abundance of submerged plants (e.g., at sites E4, E9, and E13); specifically, the contribution of C2 to the autochthonous components was greater. Therefore, the contribution of submerged plants to C2 cannot be ignored, and this may explain the high proportion of C2 in the water column during winter. In winter, the decay of submerged plants releases a large quantity of this component, decreasing the degradation rate of planktonic bacteria, and leading to the long-term retention of C2

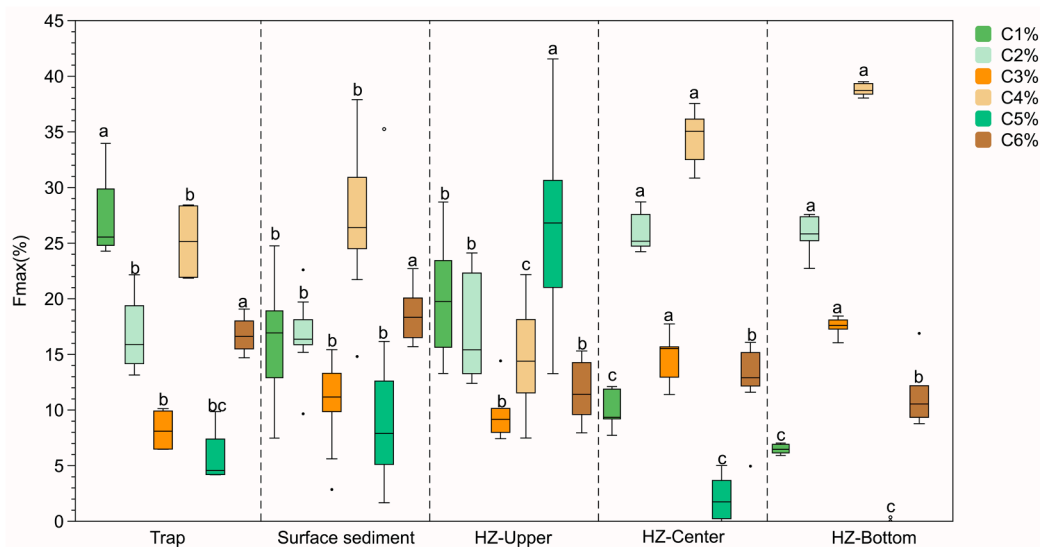


Fig. 7. Box plots showing the Vertical variation of the components from the trap sediments to the core sediments. Vertical variation of six components after standardization (one-way ANOVA with LSD test,  $p < 0.05$ ). Different lowercase letters indicate that the same component varies significantly between different sediments.



in the water. The characteristics of submerged plants are similar to those of terrestrial vegetation. Previous studies have attributed this complex component to allochthonous OM, which leads to the neglect of the autochthonous OM contribution in sediments. The stability rate of allochthonous OM was maintained at approximately ~30 – 50 % because it is the product of the repeated utilization of land plants by soil microorganisms. Thus, allochthonous OM has a relatively constant stability rate. Based on the above analysis, the correct interpretation of the mineralised products of OM from different sources is vital for the comprehensive exploration of the lake carbon sink.

#### 4.3. Contribution of autochthonous OC to total OC burial

We estimated the proportion of auto-DOM from the trap sediments to the surface and core sediments using the proportion of components based on PARAFAC analysis. The mean contributions were  $\sim 49.9 \pm 5.84$ ,  $\sim 43.4 \pm 8.84$ , and  $\sim 44.5 \pm 14.41$  % in the trap sediments, surface sediments, and core sediments, respectively. We also estimated the proportions of autochthonous OM based on C/N ratios, whose values were  $\sim 56.7 \pm 5.62$ ,  $\sim 40.9 \pm 14.26$ , and  $\sim 48.4 \pm 6.04$  % in the trap sediments, surface sediments, and core sediments, respectively. These results are considerably different from those from boreal lakes in southeast Sweden (Guillemette et al., 2017). This may be because of the different end-member choices used compared to our study. We calculated the autochthonous contributions using two methods (Fig. 8). Although we did not consider terrestrial plants as end-members when calculating the contribution of autochthonous DOC to the C/N ratio, the results were close to those obtained by the PARAFAC analysis. In the analysis of fluorescence components, component C2 in our study contributed significantly to the autochthonous component, and it may have been neglected in previous studies of carbon sinks.

Auto-DOM accounted for 42–68 % of the total DOM in the vertical direction (i.e., water  $\rightarrow$  trap sediments  $\rightarrow$  surface sediments  $\rightarrow$  core sediments) (Fig. S5), rather than being rapidly utilised and returned to circulation, as was previously thought (Guillemette et al., 2016). A study of Fuxian Lake showed that it has a higher proportion of auto-DOM (60–68 %, calculated using an n-alkanes calculation method) compared to Erhai Lake (He et al., 2021). We believe that the basin area and residence time are important reasons for this difference. (Wan et al., 2003; He et al., 2020). The effective burial of autochthonous OM plays a key role in future carbon sink regulation. Li et al. (2022) estimated the proportion of autochthonous OM in core sediments in eutrophic Lake Dianchi using  $\delta^{13}\text{C}_{\text{org}}$  and PARAFAC analysis, with values of

16.44–61.25 %. Although the proportion of autochthonous OM in the surface core sediments was relatively high, the content of autochthonous OM retained over a long timescale was low. Notably, different lakes have different autochthonous OM retention capacities owing to their different environmental characteristics. Therefore, understanding the mechanism of the effective preservation of OM produced by primary production in the sediments of inland lakes requires detailed studies which may also reveal why RDOM in water can be stored as particles in sediments over a long interval, as observed in the present study.

Previous studies have found that refractory DOM compounds with carboxyl and hydroxyl groups tend to undergo ligand exchange with metals (Wang et al., 2021), and that the content of autochthonous OM in sediments is not only related to the primary productivity but also to the phytoplankton community structure and inputs of lithogenic minerals (Galy et al., 2007; Wei et al., 2022), which is similar to the “ballast effect” in the ocean (Klaas and Archer, 2002). Large quantities of catchment-derived carbonates enter Erhai Lake, and there is a high content of lithogenic materials (e.g., clay minerals, quartz) in the lake water (Wan et al., 2003). We found that planktonic algae in water mainly comprise diatoms (data from Lai et al., 2022), which can be more effectively adsorbed by clay minerals and flocculants than cyanobacteria, producing larger POM (Avnimelech et al., 1982; Hamm, 2002). Previous studies showed that the autochthonous OM in reservoirs dominated by diatoms was more likely to be incorporated in the sediments than in lakes enriched in cyanobacteria (Wei et al., 2022). Diatoms have a more recalcitrant organic component, glycine, which is less likely to degrade in sediments (Hecky et al., 1973). In the soil carbon cycle,  $\text{Ca}^{2+}$  is known to play a significant role in the stabilisation of OC by exchanging its hydration shell and creating inner sphere complexes with organic functional groups (Rowley et al., 2018). We suggest that this may explain the burial of C2 as particles in Erhai Lake. The environmental characteristics of karst aquatic systems were also an important reason for us to investigate the vertical changes in RDOM in inland water bodies. This phenomenon was observed at Puding Karst Test site, and the system with a high  $\text{Ca}^{2+}$  concentration was found to be more conducive to the burial of C2 (Xia et al., 2022).

## 5. Conclusion

We have investigated the temporal and spatial variations of OM in Erhai Lake. We identified two autochthonous components (C1, C2) and two allochthonous components (C3, C4) in the water. We found that C2 may be the RDOM in Erhai lake, and high concentrations of C2 in the water in winter and spring indicated that these two seasons provide favourable conditions for RDOM burial. Three autochthonous components (C1, C2, C5) and three allochthonous components (C3, C4, C6) were identified in the lake sediments using Parallel Factor (PARAFAC) analysis. C2 was preserved in the form of RDOM in the vertical direction (i.e., water  $\rightarrow$  trap sediments  $\rightarrow$  surface sediments  $\rightarrow$  core sediments). Combined with the vertical changes in C/N ratio and  $\delta^{13}\text{C}_{\text{org}}$ , C2 plays a vital role in the stability of autochthonous OM and the contribution of autochthonous OM is similar to that of allochthonous OM in the sediments of Erhai Lake. At the same time, the specific environmental conditions may lead to the more stable preservation of DOM. Further studies are needed to study the dilution effect in inland water bodies and to explore the mechanism and contribution of autochthonous OC burial on a geological scale.

### CRedit authorship contribution statement

**Fan Xia:** Writing – original draft, Software, Visualization, Data curation. **Zaihua Liu:** Conceptualization, Methodology, Supervision, Writing – review & editing. **Min Zhao:** Data curation, Supervision, Formal analysis, Software, Writing – review & editing. **Haibo He:** Data curation, Investigation. **Qiufang He:** Data curation, Software. **Chaowei Lai:** Investigation. **Xuejun He:** Investigation. **Zhen Ma:** Investigation.

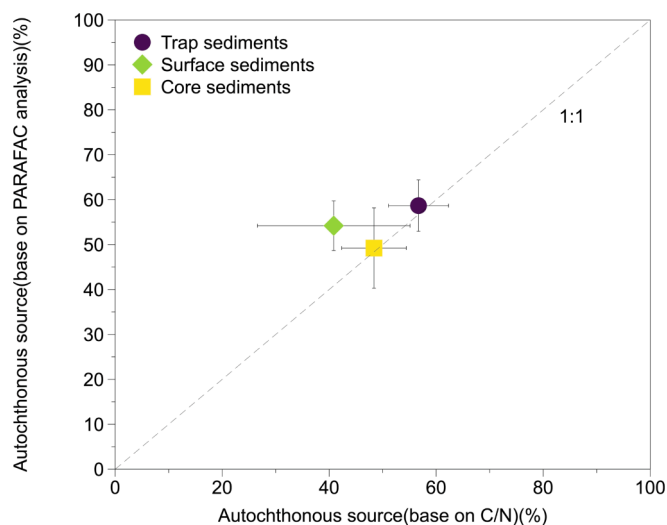


Fig. 8. Comparison of autochthonous OM contributions calculated using two different methods (C/N ratio and PARAFAC analysis).

**Yang Wu:** Investigation. **Song Ma:** Investigation.

### Declaration of Competing Interest

The authors declare that they have no known competing financial interests or personal relationships that could have appeared to influence the work reported in this paper.

### Data availability

No data was used for the research described in the article.

### Acknowledgements

This study was financially supported by the National Natural Science Foundation of China (42130501, 42141008, 42177248, and 41921004), and the Strategic Priority Research Program of Chinese Academy of Sciences (XDB40020000). We thank Jan Bloemendal for polishing the manuscript.

### Appendix A. Supplementary data

Supplementary data to this article can be found online at <https://doi.org/10.1016/j.jhydrol.2023.130407>.

### References

- Arrieta, J.M., Mayol, E., Hansman, R.L., Herndl, G.J., Dittmar, T., Duarte, G.M., 2015. Dilution limits dissolved organic carbon utilization in the deep ocean. *Science* 348 (6232), 331–333.
- Avnimelech, Y., Troeger, B.W., Reed, L.W., 1982. Mutual flocculation of algae and clay: evidence and implications. *Science* 216 (4541), 63–65.
- Chen, Q., Chen, F., Gonsior, M., Li, Y.Y., Wang, Y., He, C., Cai, R.H., Xu, J.X., Wang, Y.M., Xu, D.P., Sun, J., Zhang, T., Shi, Q., Jiao, N.Z., Zheng, Q., 2021. Correspondence between DOM molecules and microbial community in a subtropical coastal estuary on a spatiotemporal scale. *Environ. Int.* 154, 106558.
- Cole, J.J., Prairie, Y.T., Caraco, N.F., McDowell, W.H., Tranvik, L.J., Striegl, R.G., Duarte, C.M., Kortelainen, P., Downing, J.A., Middelburg, J.J., Melack, J., 2007. Plumbing the global carbon cycle: Integrating inland waters into the terrestrial carbon budget. *Ecosystems* 10, 172–185.
- Dittmar, T., 2015. Reasons behind the long-term of dissolved organic matter, in edited by D. A. Hansell and C. A. Carlson, *Biogeochemistry of Marine Dissolved Organic Matter*, pp. 369–388, Elsevier, London.
- Feeley, R.A., Doney, S.C., Cooley, S.R., 2009. Ocean acidification: present conditions and future changes in a high-CO<sub>2</sub> world. *Oceanography* 22 (4), 36–47.
- Filippi, M.L., Talbot, M.R., 2005. The palaeolimnology of northern Lake Malawi over the last 25 ka based upon the elemental and stable isotopic composition of sedimentary organic matter. *Quaternary Sci. Rev.* 24, 1303–1328.
- Galy, V., France-Lanord, C., Beyssac, O., Faure, P., Kudrass, H., Palhol, F., 2007. Efficient organic carbon burial in the Bengal fan sustained by the Himalayan erosional system. *Nature* 450, 407–410.
- Gudasz, C., Bastviken, D., Premke, K., Steger, K., Tranvik, L.J., 2012. Constrained microbial processing of allochthonous organic carbon in boreal lake sediments. *Limnol. Oceanogr.* 57 (1), 163–175.
- Guillemette, F., McCallister, L.S., Giorgio, D.P., 2016. Selective consumption and metabolic allocation of terrestrial and algal carbon determine allochthony in lake bacteria. *ISME J.* 10, 1373–1382.
- Guillemette, F., Wachenfeldt, E.V., Kothawala, D.N., Bastviken, D., Tranvik, L.J., 2017. Preferential sequestration of terrestrial organic matter in boreal lake sediments. *J. Geophys. Res. Biogeosci.* 122, 863–874.
- Hamdan, M., Bystrom, P., Hotchkiss, E.R., Al-Haidarey, M.J., Ask, J., Karlsson, J., 2018. Carbon dioxide stimulates lake primary production. *Sci. Rep.* 8, 10878.
- Hamm, C.E., 2002. Interactive aggregation and sedimentation of diatoms and clay-sized lithogenic material. *Limnol. Oceanogr.* 47 (6), 1790–1795.
- Hansell, D.A., Carlson, C.A., Schlitzer, R., 2012. Net removal of major marine dissolved organic carbon fractions in the subsurface ocean. *Global Biogeochem.* 26, GB1016.
- Hanson, P.C., Pace, M.L., Carpenter, M.L., Cole, J.J., Stanley, E.H., 2014. Integrating landscape carbon cycling: Research needs for resolving organic carbon budgets of lakes. *Ecosystems* 1–13.
- Hassan, K.M., Swinehart, J.B., Spalding, R.F., 1997. Evidence for Holocene environmental change from C/N ratios and  $\delta^{13}\text{C}$  and  $\delta^{15}\text{N}$  values in Swan Lake sediments, western Sand Hills, Nebraska. *J. Paleolimnol.* 18, 121–130.
- He, D., Li, P.H., He, C., Wang, Y.T., Shi, Q., 2022. Eutrophication and watershed characteristics shape changes in dissolved organic matter chemistry along two river-estuarine transects. *Water Res.* 214, 118196.
- He, H.B., Liu, Z.H., Chen, C.Y., Wei, Y., Bao, Q., Sun, H.L., Yan, H., 2020. The Sensitivity of the Carbon Sink by Coupled Carbonate Weathering to Climate and Land-Use Changes: Sediment Records of the Biological Carbon Pump Effect in Fuxian Lake, Yunnan, China, during the Past century. *Sci. Total Environ.* 720, 137539.
- He, Q.F., Xiao, Q., Fan, J.X., Zhao, H.J., Cao, M., Zhang, C., Jiang, Y.J., 2021. Excitation-emission matrix fluorescence spectra of chromophoric dissolved organic matter reflected the composition and origination of dissolved organic carbon in Lijiang River. Southwest China. *J. Hydrol.* 598, 126240.
- Hecky, R.E., Mopper, K., Kilham, P., Degens, E.T., 1973. The amino acid and sugar composition of diatom cell-walls. *Mar. Biol.* 19 (4), 323–331.
- Hobbie, J.E., 1988. A comparison of the ecology of planktonic bacteria in fresh and salt water. *Limnol. Oceanogr.* 33, 750–764.
- Javadinejad, S., Eslamian, S., Ostad-Ali-Askari, K., 2019. Investigation of monthly and seasonal changes of methane gas with respect to climate change using satellite data. *Appl. Water Sci.* 9, 180.
- Jiao, N.Z., Herndl, G., Hansell, D., Ronald, B., Gerhard, K., Steven, W.W., David, L.K., Markus, G.W., Luo, T.W., Chen, F., Farooq, A., 2010. Microbial production of recalcitrant dissolved organic matter: Long-term carbon storage in the global ocean. *Nat. Rev. Microbiol.* 8, 593–599.
- Jiao, N.Z., Robinson, C., Azam, F., Thomas, H., Baltar, F., Dang, H., et al., 2014. Mechanisms of microbial carbon sequestration in the ocean-future research directions. *Biogeo. Sci.* 11 (19), 5285–5306.
- Kida, M., Kojima, T., Tanabe, Y., Hayashi, K., Kudoh, S., Maie, N., Fujitake, N., 2019. Origin, distributions, and environmental significance of ubiquitous humic-like fluorophores in Antarctic lakes and streams. *Water Res.* 163, 114910.
- Klaas, C., Archer, D.E., 2002. Association of settling organic matter with various types of mineral ballast in the deep sea: implications for the rain ratio. *Glob. Biogeochem. Cycles* 16 (4), 1116.
- Kothawala, D.N., Stedmon, C.A., Müller, R.A., Weyhenmeyer, G.A., Köhler, S.J., Tranvik, L.J., 2014. Controls of dissolved organic matter quality: Evidence from a large-scale boreal lake survey. *Global Change Biol.* 1101–1114.
- Lai, C.W., Ma, Z., Liu, Z.H., Sun, H.L., Yu, Q.C., Xia, F., He, X.J., Bao, Q., He, H.B., Han, Y. Q., Liu, X., 2022. Alleviating eutrophication by reducing the abundance of Cyanophyta due to dissolved inorganic carbon fertilization: Insights from Erhai Lake, China. *J. Environ. Sci.* 6, (<https://doi.org/10.1016/j.jes.2022.10.030>).
- Lamb, A.L., Wilson, G.P., Leng, M.J., 2006. A review of coastal palaeoclimate and relative sea-level reconstructions using  $\delta^{13}\text{C}$  and C/N ratios in organic material. *Earth Sci. Rev.* 75, 29–57.
- Legendre, L., Rivkin, R.B., Weinbauer, M.G., et al., 2015. The microbial carbon pump concept: potential biogeochemical significance in the globally changing ocean. *Prog. Oceanogr.* 134, 432–450.
- Lehmann, M.F., Bernasconi, S.M., Barberi, A., Mckenzie, J.A., 2002. Preservation of organic matter and alteration of its carbon and nitrogen isotope composition during simulated and in situ early sedimentary diagenesis. *Geochim. Cosmochim. Acta.* 66, 3573–3584.
- Li, S.D., Fang, J., Zhu, X.S., Spencer, R.G.M., Salgado, X.A.A., Deng, Y.C., Huang, T., Yang, H., Huang, C.C., 2022. Properties of sediment dissolved organic matter respond to eutrophication and interact with bacterial communities in a plateau lake. *Environ. Pollut.* 301, 118996.
- Liu, C., Li, Z., Berhe, A.A., Xiao, H., Liu, L., Wang, D., Peng, H., Zeng, G., 2019. Characterizing dissolved organic matter in eroded sediments from a loess hilly catchment using fluorescence EEM-PARAFAC and UV-Visible absorption: insights from source identification and carbon cycling. *Geoderma* 334, 37–48.
- Liu, Z.H., Zhao, M., Sun, H.L., Yang, R., Chen, B., Yang, M.X., Zeng, Q.R., Zeng, H.T., 2017. “Old” carbon entering the South China Sea from the carbonate-rich Pearl River Basin: Coupled action of carbonate weathering and aquatic photosynthesis. *Appl. Geochem.* 78, 96–104.
- Liu, Z.H., Yan, H., Zeng, S.B., 2021. Increasing autochthonous production in inland waters as a contributor to the missing carbon sink. *Front Earth Sci.* 9, 620513.
- Longhurst, A., Harrison, W., 1989. The biological pump: profiles of plankton production and consumption in the upper ocean. *Prog. Oceanogr.* 22 (1), 47–123.
- McIntyre, A.M., Gueguen, C., 2013. Binding interactions of algal-derived dissolved organic matter with metal ions. *Chemosphere* 90 (2), 620–626.
- Meyers, P.A., 1997. Organic geochemical proxies of paleoceanographic, paleolimnological and paleoclimatic processes. *Org. Geochem.* 27, 213–250.
- Meyers, P.A., Ishiwatari, R., 2003. Applications of organic geochemistry to paleolimnological reconstructions: a summary of examples from the Laurentian Great Lakes. *Org. Geochem.* 34, 261–289.
- Nafchi, R.F., Samadi-Boroujeni, H., Vanani, H.R., et al., 2021. Laboratory investigation on erosion threshold shear stress of cohesive sediment in Karkheh Dam. *Environ. Earth Sci.* 80, 681.
- Rowley, M.C., Grand, S., Verrecchia, É.P., 2018. Calcium-mediated stabilisation of soil organic carbon. *Biogeochemistry* 137, 27–49.
- Sarmento, H., Morana, C., Gasol, J., 2016. Bacterioplankton niche partitioning in the use of phytoplankton-derived dissolved organic carbon: quantity is more important than quality. *ISME J.* 10, 2582–2592.
- Schallenberg, M., Kalf, J., 1993. The ecology of sediment bacteria in lakes and comparisons with other aquatic ecosystems. *Ecology.* 74, 919–934.
- Schmidt, F., Elvert, M., Koch, B.P., Witt, M., Hinrichs, K.U., 2009. Molecular characterization of dissolved organic matter in pore water of continental shelf sediments. *Geochim. Cosmochim. Acta* 73 (11), 3337–3358.
- Schmidt, M.W., Torn, M.S., 2011. Persistence of soil organic matter as an ecosystem property. *Nature* 478 (7367), 49–56.
- Stedmon, C., Markager, S., 2005. Resolving the variability in dissolved organic matter fluorescence in a temperate estuary and its catchment using PARAFAC analysis. *Limnol. Oceanogr.* 50, 686–697.
- Talebmorad, H., Ostad-Ali-Askari, K., 2022. Hydro geo-sphere integrated hydrologic model in modeling of wide basins. *Sustain. Water Resour. Manag.* 8, 118.

- Tranvik, L.J., Downing, J.A., Cotner, J.B., Loiselle, S.A., Striegl, R.G., Ballatore, T.J., Dillon, P., Finlay, K., Fortino, K., Knoll, L.B., 2009. Lakes and reservoirs as regulators of carbon cycling and climate. *Limnol. Oceanogr.* 54, 2298–2314.
- Visser, P.M., Verspagen, J.M., Sandrini, G., Stal, L.J., Matthijs, H.C., Davis, T.W., Paerl, H.W., Huisman, J., 2016. How rising CO<sub>2</sub> and global warming may stimulate harmful cyanobacterial blooms. *Harmful. Algae.* 54, 145–159.
- Wan, G.J., Bai, Z.G., Qing, H., Mather, J.D., Huang, R.G., Wang, H.R., Tanga, D.G., Xiao, B.H., 2003. Geochemical records in recent sediments of Lake Erhai: implications for environmental changes in a low latitude–high altitude lake in southwest China. *J. of Asian Earth Sci.* 21, 489–502.
- Wang, H., Li, Z., Zhuang, W.E., Hur, J., Yang, L., Wang, Y., 2020. Spectral and isotopic characteristics of particulate organic matter in a subtropical estuary under the influences of human disturbance. *J. Mar. Syst.* 203, 103264.
- Wang, K., Pang, Y., Gao, C., Chen, L., He, D., 2021. Hydrological management affected dissolved organic matter chemistry and organic carbon burial in the Three Gorges Reservoir. *Water Res.* 199, 117195.
- Wei, Y., Yan, H., Liu, Z.H., Han, C.H., Ma, S., Sun, H.L., Bao, Q., 2022. The ballast effect controls the settling of autochthonous organic carbon in three subtropical karst reservoirs. *Sci. Total Environ.* 818, 151736.
- Wolfe, A.P., Kaushal, S.S., Fulton, J.R., McKnight, D.M., 2002. Spectrofluorescence of sediment humic substances and historical changes of lacustrine organic matter provenance in response to atmospheric nutrient enrichment. *Environ. Sci. Technol.* 36, 3217–3223.
- Xia, F., Liu, Z.H., Zhao, M., Li, Q., Li, D., Cao, W.F., Zeng, C., Hu, Y.D., Chen, B., Bao, Q., Zhang, Y., He, Q.F., Lai, C.W., He, X.J., Ma, Z., Han, Y.Q., He, H.B., 2022. High stability of autochthonous dissolved organic matter in karst aquatic ecosystems: Evidence from fluorescence. *Water Res.* 220, 118723.
- Yamashita, Y., Tanoue, E., 2008. Production of bio-refractory fluorescent dissolved organic matter in the ocean interior. *Nature Geosci.* 1, 579–582.
- Zeebe, R.E., Wolf-Gladrow, D.A., 2001. CO<sub>2</sub> in seawater: equilibrium, kinetics, isotopes. Elsevier, Amsterdam 65 (3).
- Zhao, Z., Gonsior, M., Luek, J., Timko, S., Ianiri, H., Hertkorn, N., Schmitt-Kopplin, P., Fang, X.T., Zeng, Q.L., Jiao, N.Z., Chen, F., 2017. Picocyanobacteria and deep-ocean fluorescent dissolved organic matter share similar optical properties. *Nat. Commun.* 8, 15284.
- Zhao, H., Zhao, H., Wang, S., Zhao, L., Qiao, Z.C., 2020. Coupling characteristics and environmental significance of nitrogen, phosphorus and organic carbon in the sediments of Erhai Lake. *Environ Sci Pollut Res.* 27, 19901–19914.
- Zhou, L., Zhou, Y., Hu, Y., Cai, J., Liu, X., Bai, C., Tang, X.M., Zhang, Y.L., Jang, K.S., Spencer, R.G.M., 2019. Microbial production and consumption of dissolved organic matter in glacial ecosystems on the Tibetan plateau. *Water Res.* 160, 18–28.
- Zhou, L., Zhou, Y., Tang, X., Zhang, Y., Jeppesen, E., 2021. Resource aromaticity affects bacterial community successions in response to different sources of dissolved organic matter. *Water Res.* 190, 116776.